Bauhaus-Universität Weimar
20.-22. September 2022
BauSIM2022 in Weimar
ibpsa

LOCAL ROOM-SIDE HEAT TRANSFER OF AN OFFICE ROOM WITH DIFFERENT HEATING STRATEGIES

Zhenming Peng[1], Svenja Carrigan[1], Oliver Kornadt[1]
[1] *Technische Universität Kaiserslautern, Germany, E-Mail: zhenming.peng@bauing.uni-kl.de*

Abstract

This paper focuses on ANSYS Fluent simulations of the effect of floor heating, mixing ventilation, furniture, room geometry and their combinations on the interior heat transfer coefficient (HTC) of a typical office room. The results show an inhomogeneous distribution of the HTC on the exterior walls. HTC values are generally below the German standardised value for thermal protection, leading to an overestimation of the heat transfer losses by the standardised value. However, compared to the standardised value for the prevention of mould growth, the minimum surface averaged HTC behind closets is 63 % lower, potentially leading to condensation.

Introduction

The basis for the prediction of the thermal and hydric behaviour of building components are the heat transfer processes from the environment through the building components. The material properties are one of the key parameters in this process. Moreover, the thermal and hydric conditions as well as the airflow of the indoor/outdoor environment play an important role in determining the heat transfer from the indoor environment to the building envelope and from the building envelope to the outdoor environment.

This paper focuses on the room side heat transfer. The heat transfer between the indoor environment and the interior surfaces can be generally divided into two processes, convective and radiative heat transfer. The heat exchange through these processes is usually calculated based on the convective heat transfer coefficient (CHTC) h_{con} and the radiative heat transfer coefficient (RHTC) h_{rad}. They are defined as:

$$h_{con/rad} = \frac{q}{T_s - T_r} \quad (1)$$

where q is the convective or radiative heat flux, T_s is the surface temperature and T_r is the reference temperature.

The RHTC can be derived by well-established analytical and numerical models. The approach for CHTC is much less precise, since information about different room configurations that affect the airflow patterns, such as the room conditioning strategies, room geometry as well as furniture, are necessary for the modelling of the convective heat transfer. In contrast to a detailed modelling, general combined values of CHTC and RHTC are used for different calculation purposes in Germany. For energy calculations, depending on the direction of the heat flux, the values range from 5.88 to 10 W/m²K (DIN EN ISO 6946, 2018). For ensuring the sufficient thermal insulation to avoid mould growth, the value is 4 W/m²K (DIN 4108-2, 2013) without any furniture and 1 W/m²K behind build-in closets (DIN 4108-8, 2010). These values assume a uniform room temperature and neglect the effect of the room configurations discussed above.

In recent years, many CHTC models were developed for different room configurations (Obyn & van Moeseke, 2015). The studies can be generally arranged into three categories: natural, forced and mixed convection. Conventional room conditioning strategies, such as floor heating and radiator as well as ventilation systems were investigated. Up to 11.5 % deviation of the simulated energy consumption between simulations applying different CHTC models was found by implementing the models for different types of room conditioning (Peng et al., 2022). However, most studies were carried out in an empty room under nearly adiabatic conditions. Realistic building constructions were not considered, which could lead to a great deviation of the HTC due to local temperature inhomogeneities caused by thermal bridges and thermal masses, such as the walls/ceiling and the furniture. Furthermore, furniture located close to the walls obstruct the airflow behind it, which also affects the HTC.

In this work simulation studies of the room side heat transfer in an office room built in common concrete construction were performed. The purpose of this study was on the one hand to numerically investigate the indoor airflow distributions effected by geometrical thermal bridges, room furnishings and room conditioning strategies. The effect of floor heating, mixing ventilation, furniture, room geometry and their combinations on the interior heat transfer was investigated. On the other hand, this study aimed to quantify the difference between the numerical determined heat transfer coefficient and the normative values. Therefore, both surface averaged and local

heat transfer coefficient of the studied simulation variables are presented.

Methodology

The Computational Fluid Dynamics (CFD) software FLUENT was used for the simulation (ANSYS Inc). The geometry of the investigated room is shown in Figure 1. The room has internal dimensions of 4.2 m in length, 3 m in height and 3 m in width. To investigate the effect of the furniture on the heat transfer in the room, a closet with dimensions of 2 m × 2 m × 0.4 m is placed at the corner with a distance of 1 cm to the exterior walls. As for the simulation variables with a mixing ventilation system, the air inlet and outlet with a dimension of 30 cm in width and 10 cm in height are placed at an internal wall with a distance of 0.6 m to the ceiling and floor, respectively. The air inlet and outlet were dimensioned based on an air change rate of 2.5 h^{-1} and 2 m/s inlet air velocity.

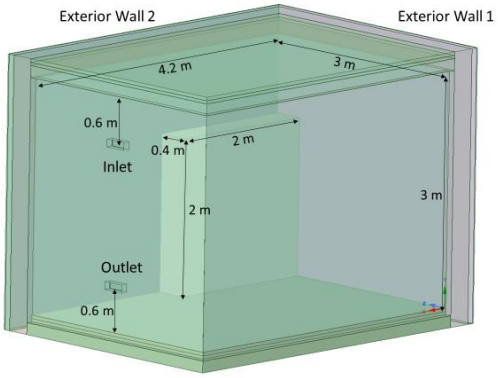

Figure 1: Room geometry.

The exterior wall construction from the inside surface is 15 mm plaster, 300 mm concrete, 85 mm insulation layer and 15 mm plaster with a total U-value of 0.358 W/m²K. The internal walls consist of 15 mm plaster, 175 mm concrete and 15 mm plaster. The internal floor and ceiling have 45 mm screed, 40 mm insulation layer and 150 mm concrete.

Following heating and ventilation configuration cases were investigated:

- C1: floor heating system
- C2: floor heating system + a closet at the corner of the exterior walls
- C3: mixing ventilation system
- C4: mixing ventilation system + a closet at the corner of the exterior walls
- C5: floor heating system + mixing ventilation system
- C6: floor heating system + mixing ventilation system + a closet at the corner of the exterior walls

Solution procedure

Since the studied cases are conjugate convective heat transfer problems, the fluid and solid domains were coupled in the simulations. The energy equation was solved for the solid domain. As for the fluid domain, the continuity and momentum conservation equation as well as the energy equation were solved. To capture the buoyancy effect of the airflow in a closed domain, the ideal gas law was applied. In addition, extra transport equations are necessary to solve the turbulence in the airflow and the radiation exchange between surfaces.

For a detailed investigation of the convective heat transport, the viscous sublayer should be solved to capture the near wall heat transfer behaviour and temperature gradient accurately. k-ω (kinetic energy - specific energy dissipation rate) based turbulence models provide higher accuracy at the near wall region in comparison to the k-ε (kinetic energy - energy dissipation rate) based models, as in k-ω based models the viscous sublayer is directly solved without using the approximated wall functions or treatments. Furthermore, k-ω based models have also higher accuracy when separation in the flow field occurs (Apsley & Leschziner, 2000). However, the k-ε based models provide an accurate result in the far field. To combine the advantages of the k-ε based and k- ω based models, the Shear Stress Transport (SST) k-ω model implements the k-ω model in the near wall region and k-ε model in the far field. Several studies have shown accurate predictions of the flow behaviour by using this model in cases of natural, force and mixed convection in closed spaces (Cheng et al., 2005; Stamou & Katsiris, 2006; Zhang et al., 2007). Thus, the SST k-ω model was selected.

The radiation exchange between surfaces was incorporated using the surface to surface (S2S) model.

A three-dimensional structured hexahedral conformal grid was generated for the studied cases. In order to properly solve the viscous sublayer, the first grid cell to the walls was refined to keep the wall y+ value under 1. In addition, further 12 layers with a growth rate of 1.2 based on the first grid cell were generated to solve the full boundary layers. Figure 2 shows an example of the near wall region computational grid for C2. The same approach was applied for all cases.

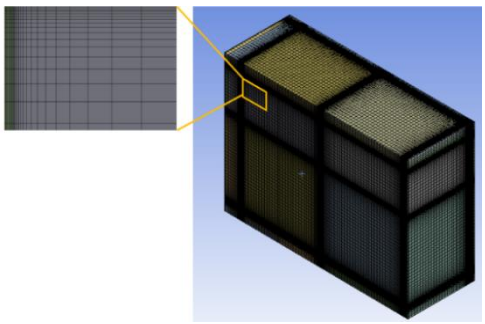

Figure 2: Example of the generated grid near the exterior wall 1 and the ceiling (C2). The figure on the right shows half of the room vertically sliced from the centre of the exterior wall 1.

Boundary conditions

The internal building components were treated as adiabatic. A constant outdoor temperature of -5 °C and an external heat transfer coefficient of 25 W/m²K were set for the outer surfaces of the exterior wall 1 (W1) and 2 (W2). For C5 and C6 the inlet air temperature was kept at 20 °C. The floor temperature in C1, C2, C5 and C6 as well as the inlet air temperature in C3 and C4 were adjusted to keep the average room temperature at 20 °C. At the inlet, the turbulence intensity was set at 5 % with an air velocity of 2 m/s. The average static pressure at the outlet is set to the atmospheric pressure. The emissivity of surfaces is 0.9 and it is assumed that all surfaces are grey.

Convergence criteria

Convergence with residuals targeted at 10^{-3} for continuity, velocity, k and ω as well as 10^{-7} for energy was achieved. The flow rate at the middle of the room, the average room air temperature, the heat flux and the temperature at the thermal bridge were monitored to evaluate the convergence behaviour and the simulation was stopped when those data appeared stable. Furthermore, grid independent solutions were obtained. This was tested using the calculation method of the grid convergence index (GCI) from (Celik et al., 2008). GCI indicates the grid convergence error due to the refinement of the mesh size, more specifically, it shows how far the result is from an asymptotic numerical solution. For this purpose, several simulations with a different global mesh size for the respective cases were performed. The mesh size was refined for each case until the GCI of the monitored data was lower than 1 %.

Simulation results and discussion

For each of the different heating systems C1 (floor heating), C3 (mixing ventilation) and C5 (combined) clearly distinguishable airflow distributions in the room were found. In C1, a buoyant vertical plume is formed near the inner wall that is located opposite to the W1. The warm airflow strikes the ceiling, moves towards the two exterior walls where it is cooled and bends downwards. In C3, the flow field is mainly momentum driven. The warm airflow from the inlet tends to be bounded to the ceiling due to the Coanda and buoyancy effect. The airflow is then cooled by the exterior walls, mixes with the air at the lower part of the room, moves towards the outlet and partially recirculates to the upper part of the room. Due to the forced ventilation in C3, the average air velocity is higher at 0.10 m/s versus 0.05 m/s in C1. The major difference in C5 compared to C3 is that the airflow in the lower region of the room shows a stronger recirculation to the upper region due to the buoyancy effect of the heated airflow near the floor, resulting in the highest average air velocity of 0.16 m/s for all of the cases.

The closet in the room (C2, C4, C6) doesn't have a significant effect on the overall airflow distribution. However, the local airflow near the closet is affected, especially at the edges of the closet where a velocity jump was found. The velocity changes rapidly from small to large values away from the closet edge towards the exposed surface.

Different room configurations have a large effect on the heat transfer in the room. Figures 3 a-f show the derived local total (solid lines), convective (dashed lines) and radiative (dotted lines) heat transfer coefficients (h_t, h_{con}, h_{rad}) depending on the distance to the thermal bridge at the edge between W1 and W2 (L) in C1-C6. The values given at the height of 0.5 m, 1 m, 1.5 m, 2 m, 2.5 m of W1 (left) and W2 (right) are presented in red, green, yellow, pink and blue, respectively. The surface averaged total HTC for the exterior walls $\bar{h}_t$ as well as the surface averaged total HTC of the wall region behind the closet $\bar{h}_{t,closet}$ are given in Table 1. The average air temperature of the room was used in Equation 1 as the reference temperature for the determination of the heat transfer coefficients. The surface averaged heat transfer coefficients were determined using integrated average temperatures and heat fluxes.

The following values in Table 1 are significant and marked in grey: the values larger than the value of DIN EN ISO 6946, as they can lead to a higher energy demand; the values lower than the value of DIN 4108-8, as they cause lower surface temperatures.

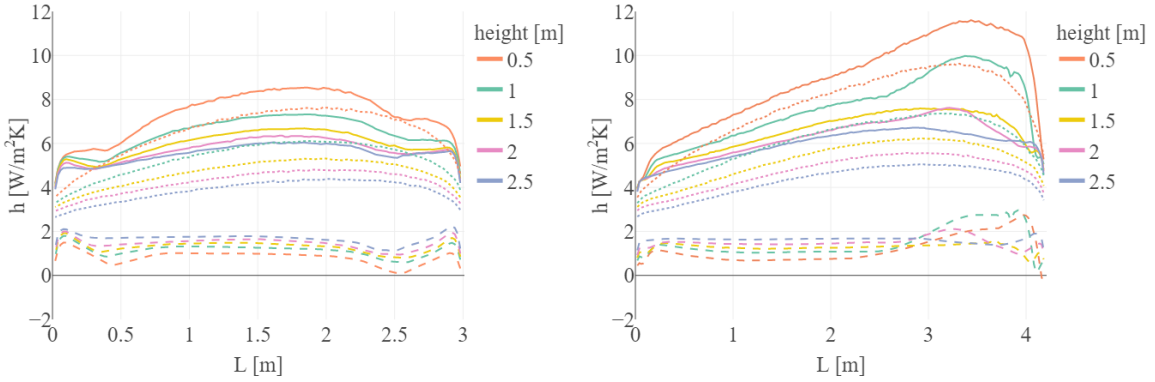

(a)

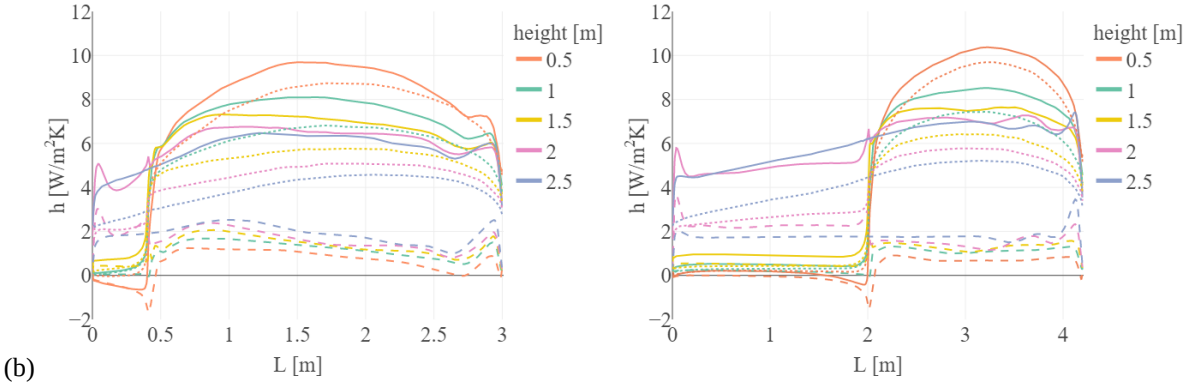
h [W/m²K]
L [m]
height [m]
0.5
1
1.5
2
2.5

(b)

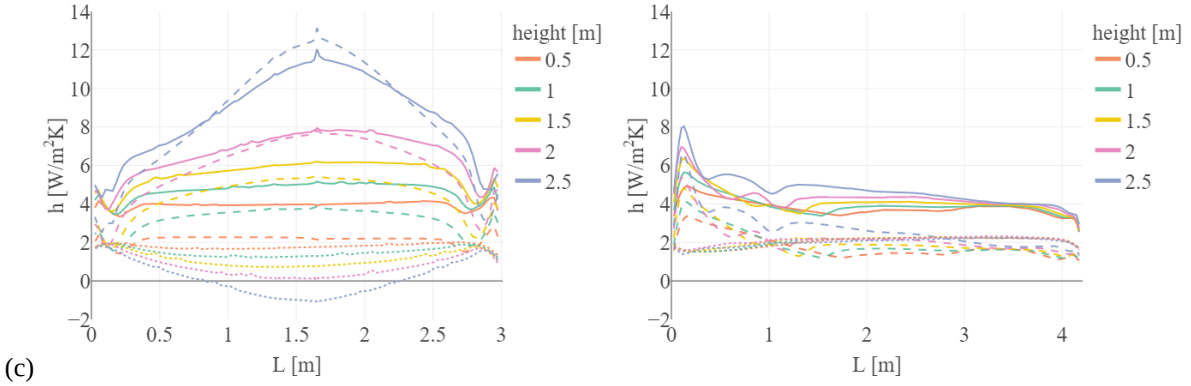
h [W/m²K]
L [m]
height [m]
0.5
1
1.5
2
2.5

(c)

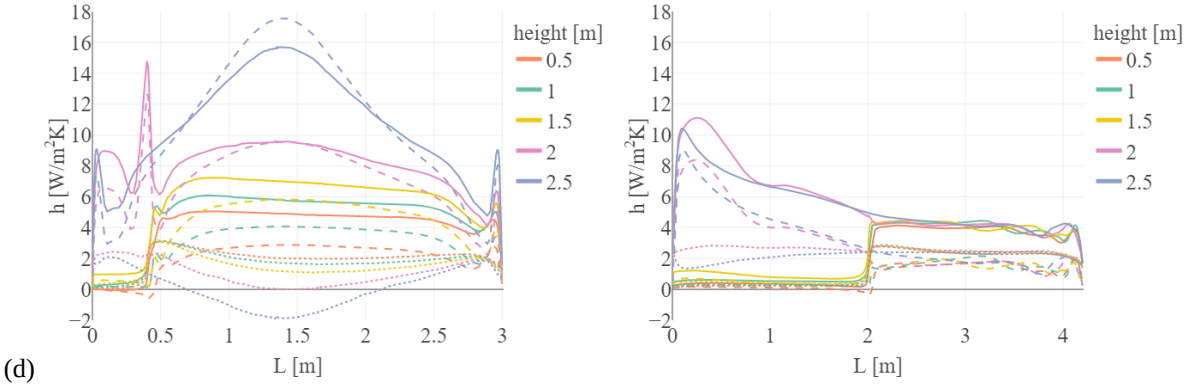
h [W/m²K]
L [m]
height [m]
0.5
1
1.5
2
2.5

(d)

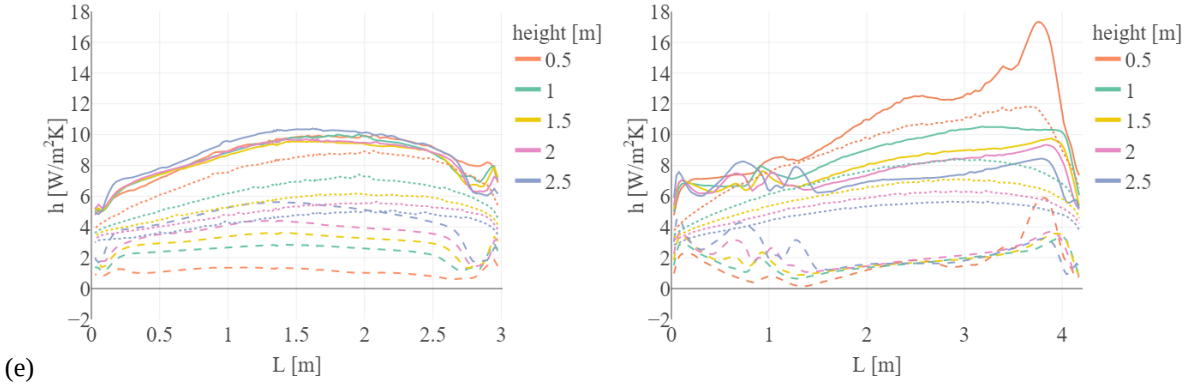
h [W/m²K]
L [m]
height [m]
0.5
1
1.5
2
2.5

(e)

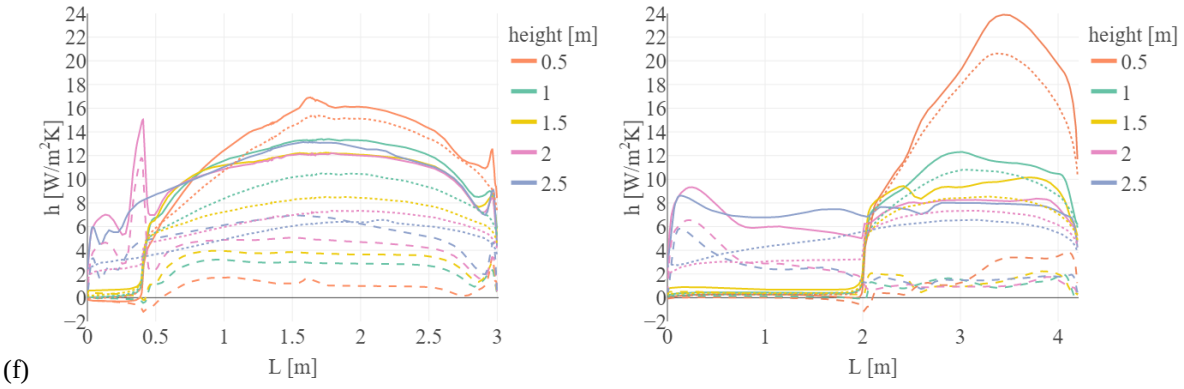

(f)

Figure 3: h_t, h_{con}, h_{rad} (solid, dashed, dotted lines) for the exterior walls W1 (left) and W2 (right) as a function of horizontal distance (L) from the edge between W1 and W2: (a) C1; (b) C2; (c) C3; (d) C4; (e) C5; (f) C6.

Table 1: surface averaged total HTC ($\bar{h}_t$) of exterior walls W1 and W2 as well as the surface averaged total HTC ($\bar{h}_{t,closet}$) of the wall region behind the closet. Values that are larger than the value of DIN EN ISO 6946 or lower than the value of DIN 4108-8 are marked in grey.

HTC [W/m²K]	C1	C2	C3	C4	C5	C6	DIN EN ISO 6946	DIN 4108 -2/8
	W1 | W2	W1 | W2	W1 | W2	W1 | W2	W1 | W2	W1 | W2		
$\bar{h}_t$	6.02 | 6.60	4.94 | 3.04	5.31 | 4.12	4.60 | 2.31	8.40 | 8.04	7.20 | 3.48	7.69	4
$\bar{h}_{t,closet}$	-	0.37 | 0.73	-	0.56 | 0.67	-	0.50 | 0.73	7.69	1

As shown in Table 1, in the cases without the closet, $\bar{h}_t$ reaches the maximum value in C5 with 8.40 W/m²K for W1 and 8.04 W/m²K for W2, which is 9 % and 4.6 % above the value from DIN EN ISO 6946, respectively. The lowest value was found in C3 with 4.12 W/m²K for W2. The presence of the closet lowers the HTC, resulting in a reduction of 1.81 W/m²K to 2.31 W/m²K in C4. The surface averaged total HTC of the wall behind the closet ranges from 0.37 W/m²K in C2 for W1, 63 % lower in comparison to the value in DIN 4108-8, and 0.73 W/m²K in C2 and C6 for W2.

In C1 where the room is heated only by the floor, the heat transfer at W1 and W2 is similar and dominated by the radiative heat transfer. Since the emissivity of all surfaces is assumed the same and the floor has the highest temperature, positions on the wall with a lower surface temperature and a small view factor to surfaces with higher temperature show a low RHTC. As a result, the radiative heat transfer becomes weaker as the position moves horizontally from the middle area of the wall to the edge and vertically from the bottom to the top. In addition, the RHTC at the thermal bridge is smaller than the RHTC at the corner with an internal wall (Fig. 3a). The CHTC contributes a smaller part (on average 23 %) to the h_t and shows fluctuations from 0 to 2 W/m²K.

In C3 (mixing ventilation), the heat transfer at the exterior walls depends on the location on the wall. Due to the direct impact of the airflow on the upper area of W1, the convective heat transfer contributes on average 73 % for W1 and only 49 % for W2 to the total heat transfer. As the position on W1 approaches the height of the inlet (2.4 m), the CHTC increases quickly (Fig. 3c). It is notable that the RHTC for W1 shows a reversed distribution compared to C1 and negative values at the height of the inlet. The reason is that the upper area of W1 is directly heated by the warm inlet flow, which causes this region to act as a radiative heat source. On W2, the CHTC value does not change significantly. Only at the thermal bridge is the CHTC higher than in the region near the inner wall where it is hardly influenced by the inflow. Furthermore, the RHTC for W2 is almost constant with an average value of 2.01 W/m²K.

In C5 with combined systems, the heat transfer is dominated by the radiative heat transfer with an average 66 % contribution to the total heat transfer for W1 and 74 % for W2. The CHTC distribution on the exterior walls is similar to C3 and the RHTC distribution is similar to C1. As a result, the h_t for W1 does not change remarkably at different heights, the maximum variation is 2 W/m²K at the distance of 2.9 m to the thermal bridge. For W2, a reverse flow was found at the distance about 0.5 m to the thermal bridge, resulting in an unstable heat transfer in this region (Fig. 3e).

The closet in C2, C4 and C6 weakens the heat transfer behind it significantly (Fig. 3b, d, f). The minimum local HTC was found at the lower region of the thermal bridge with 0.01 W/m²K in C2, 0.03 W/m²K

in C4 and 0.01 W/m²K in C6 (Fig. 3b, d, f). It is notable that negative values of h_t were identified for W1 and W2 below the height of 0.5 m at the region of closet edges with a distance of 0.4 m and 2 m to the edge between W1 and W2, respectively. This indicates that the wall temperatures in these areas are higher than the local air temperature, resulting to a reversed convective heat transfer. A rapid change of the CHTC was also observed at the edge of the closet, which can be attributed to the aforementioned velocity jump.

For all the cases, at the corners of the room, the laminar viscous sublayers of the walls affect each other, resulting in a small CHTC. Moreover, the transition from laminar to turbulent regions also affects the edge, which results in peak values for CHTC at the distance of around 0.08 m to the edge. Furthermore, the fluctuation of CHTC appears to be consistent with the change in turbulent kinetic energy.

Summary and conclusions

This study analysed the convective and radiative heat transfer in an office room with six different heating and ventilation configurations. The surface averaged and local heat transfer coefficients (HTCs) for the exterior walls at different heights and for the wall regions behind the closet were derived from the numerical simulations. The HTC varies greatly depending on the room conditioning strategy and positions in the room, especially at the positions where geometry changes, e.g. in edge areas.

The standardised value for the calculation of the energy demand tend to overestimate the HTC. However, in the case with a combined system of floor heating and mixing ventilation, a 9 % higher value of the surface averaged HTC was determined. This can lead to a underprediction of the energy demand when using the standardised value. For the prevention of mould growth and condensation, the standardised value for the surface area without obstruction by any furniture tends to lay on the safe side. In the cases with a closet at the thermal bridge area at the edge of the room, surface averaged HTC behind the closet ranges from 0.37 to 0.73 W/m²K. The minimum surface averaged value is 63 % lower than the standardised value to be used for an obstruction by closets. Moreover, a local HTC of almost zero was observed at lower regions of the line-shaped thermal bridge at the edge between the exterior walls behind the closet. This must be considered in the design process as it leads to a lower surface temperature compared to the standardised value, which could cause condensation and mould growth.

Acknowledgement

This research is funded by the German Research Foundation (DFG). Its support is gratefully acknowledged.

References

ANSYS Inc. Ansys Academic Research Fluent (Version Release 20.2) [Computer software].

Apsley, D. D., & Leschziner, M. A. (2000). Advanced Turbulence Modelling of Separated Flow in a Diffuser. *Flow, Turbulence and Combustion*, *63*(1/4), 81–112.

Celik, I., Ghia, U., Roache, P. J., Freitas, C., Coloman, H., & Raad, P. (2008). Procedure of Estimation and Reporting of Uncertainty Due to Discretization in CFD Applications. *Journal of Fluids Engineering*, *130*, 78001.

Cheng, H., Kurabuchi, T., & Ohba1, M. (2005). Numerical Study of Cross-Ventilation Using Two-Equation RANS. *International Journal of Ventilation*, *4*(2), 123–131.

DIN 4108-2: Thermal protection and energy economy in buildings - Part 2: Minimum requirements to thermal insulation (2013).

DIN EN ISO 6946: Building components and building elements - Thermal resistance and thermal transmittance - Calculation methods (2018).

DIN-Fachbericht 4108-8: Thermal insulation and energy economy in buildings - Part 8: Avoidance of mould growth in residential buildings (2010).

Obyn, S., & van Moeseke, G. (2015). Variability and impact of internal surfaces convective heat transfer coefficients in the thermal evaluation of office buildings. *Applied Thermal Engineering*, *87*, 258–272.

Peng, Z., Carrigan, S., & Kornadt, O. (2022). Untersuchung des Einflusses des raumseitigen konvektiven Wärmeübergangs auf den Heizenergiebedarf eines Raums mit unterschiedlichen Dämmniveaus und Wandkonstruktionen. *In: Proceedings Bauphysiktage, 2022, Germany*.

Stamou, A., & Katsiris, I. (2006). Verification of a CFD model for indoor airflow and heat transfer. *Building and Environment*, *41*(9), 1171–1181.

Zhang, Z., Zhang, W., Zhai, Z. J., & Chen, Q. Y. (2007). Evaluation of Various Turbulence Models in Predicting Airflow and Turbulence in Enclosed Environments by CFD: Part 2—Comparison with Experimental Data from Literature. *HVAC&R Research*, *13*(6), 871–886.